A Novel Missense Mutation in the Mouse Growth Hormone Gene Causes Semidominant Dwarfism, Hyperghrelinemia, and Obesity

CAROLA W. E. MEYER, DIRK KORTHAUS, WOLFGANG JAGLA, EMMANUELLE CORNALI, JOHANNES GROSSE, HELMUT FUCHS, MARTIN KLINGENSPOR, STEPHANIE ROEMHELD, MATTHIAS TSCHÖP, GERHARD HELDMAIER, MARTIN HRABÉ DE ANGELIS, AND MICHAEL NEHLS

Department of Biology/Animal Physiology (C.W.E.M., M.K., S.R., G.H.), Karl-von-Frisch Strasse, Philipps University Marburg, D-35043 Marburg, Germany; Ingenium Pharmaceuticals AG (D.K., W.J., E.C., J.G., M.N.), D-82152 Martinsried, Germany; GSF National Research Center for Environment and Health (H.F., M.H.A.), Institute of Experimental Genetics, D-85764 Oberschleissheim, Germany; Department of Psychiatry (M.T.), Obesity Research Center, University of Cincinnati–Genome Research Institute, Cincinnati, Ohio 45267-0559

The SMA1-mouse is a novel ethyl-nitroso-urea (ENU)-induced mouse mutant that carries an a→g missense mutation in exon 5 of the GH gene, which translates to a D167G amino acid exchange in the mature protein. Mice carrying the mutation are characterized by dwarfism, predominantly due to the reduction (sma1/+) or absence (sma1/sma1) of the GH-mediated peripubertal growth spurt, with sma1/+ mice displaying a less pronounced phenotype. All genotypes are viable and fertile, and the mode of inheritance is in accordance with a semidominant Mendelian trait. Adult SMA1 mice accumulate excessive amounts of sc and visceral fat in the presence of elevated plasma ghrelin levels, possibly reflecting altered energy partitioning. Our results suggest impaired storage and/or secretion of pituitary GH in mutants, resulting in reduced pituitary GH and reduced GH-stimulated IGF-1 expression. Generation and identification of the SMA1 mouse exemplifies the power of the combination of random mouse mutagenesis with a highly detailed phenotype-analysis as a successful strategy for the detection and analysis of novel gene-function relationships. (Endocrinology 145: 2531–2541, 2004)

G H, A 22-kDa PROTEIN hormone of 191 (human) or 190 (mouse) amino acids synthesized and released from the acidophil cells of the anterior pituitary gland, possesses well-documented anabolic as well as lipolytic activity (1). In humans and animals, deficiency in GH or its receptor (GHR) is characterized by dwarfism and truncal obesity, which can be reversed by GH replacement therapy (2–4). The majority of GH's growth-promoting effects are mediated by autocrine, paracrine, or endocrine actions of IGF-1, a cytokine expressed by hepatic cells and other peripheral tissues throughout development (5). Because IGF-1 also participates in negative feedback control of GH-axis activity at the level of both, the somatotroph pituitary cells as well as the hypothalamic neurocircuitry (6–8), blockade, or activation of the IGF-1 system will affect circulating GH levels and *vice versa*, whereas the precise extent to which either of the two players is essential for the control of postnatal growth is still under investigation (9, 10).

Significant progress in our understanding of the regulatory interface between growth control, energy metabolism, and fat mass regulation has been achieved by studying the recently discovered gastric hormone ghrelin, which potently stimulates GH release from the pituitary (11, 12) but also promotes the accretion of fat mass (13). When injected into mice and rats, ghrelin promotes a positive energy balance (13–15), and circulating ghrelin levels are preprandially elevated and postprandially decreased in humans and rodents, possibly representing a link between nutritional status and the neuroendocrine control of orexigenic drive, resting metabolic rate, tissue growth, and body composition.

Here we report the identification and phenotypic characterization of a novel missense mutation in the GH gene leading to semidominant dwarfism, hyperghrelinemia, and obesity. The mutation (*sma1*) was generated and identified in a large-scale, ethyl-nitroso-urea (ENU), random mouse mutagenesis program (GSF, Munich, Germany) (16, 17). This program represents a powerful phenotype-driven approach to gene-function analysis and increases existing mouse mutant resources.

Materials and Methods

ENU mutagenesis and identification of the mutant

Male mice of the C3HeB/FeJ strain were treated with ENU (160 mg/kg) at the age of 10 wk (according to Ref. 18). Treated mice were then mated to untreated female C3HeB/FeJ mice, and the resulting F1 offspring were analyzed for weight abnormalities as published previously (19). Briefly, body weight in offspring (F1) of ENU-treated males is routinely compared with a standard growth curve for wild-type C3HeB/FeJ males and females, and mice with a body weight more than 2 SDs below the standard curve are classified as small. The first ENU-derived dwarf was identified using this strategy, and dominant heri-

tability of the trait was confirmed by subsequent breeding. The new mutant mouse line was numbered SMA1, and all mice in this line were phenotyped by weighing until mapping of the mutation was performed. Animals were kept under specific pathogen-free (SPF) conditions at the GSF Research Center in accordance with the German laws of animal protection.

Mapping of the mutation

Mapping of the mutation was performed at Ingenium Pharmaceuticals (Ifacredo, France), using a standard outcross/backcross strategy to C57BL/6Jico mice in combination with microsatellite markers specific for the C3HeB/FeJ and C57BL/6Jico strain. Genomic DNA was purified from tailtips of wild-type C3HeB/FeJ and C57BL/6Jico mice as well as from C3HeB/FeJ-*sma1*/+ (F1 generation) and [(C3HeB/FeJ-*sma1*/+ × C57BL/6Jico) × C57BL/6Jico] mutant backcross mice by using the DNeasy 96 tissue kit (QIAGEN, Hilden, Germany) according to the manufacturer's protocol. PCRs were performed with fluorescent-labeled primers (MWG Biotech, Ebersberg, Germany), whose sequences were taken as previously published (Ref. 20, http://www.genome.wi.mit.edu). The PCRs were performed in a Tetrad thermal cycler PTC 225 device (MJ Research Inc., Waltham, MA.) in a 10-μl reaction volume using Pharmacia Taq-DNA polymerase (Amersham Pharmacia Biotech, Piscataway, NJ). A 4-min denaturation step was followed by 28 amplification cycles comprising each of 30 sec denaturation and 30 sec annealing at the respective temperatures (given in Ref. 20), and 30 sec extension at 72 C. Samples were labeled with different dyes (20), and products were separated on an ABI 377 DNA sequencing device (PE Applied Biosystems, Foster City, CA) using internal length standards in every lane. Analysis was done with Genescan version 3.0 and Genotyper version 2.1 software (PE Applied Biosystems).

For amplification, the nucleotide sequence of the *Mus musculus* GH gene and its promoter were taken from GenBank/EMBL database (Gen-Bank accession no. Z46663). The after GH-specific primer pairs designed by DOPE Interactiva (http://doprimer.interactiva.de) were used: 11M-Gh-F2: TCGGACCGTGTCTATGAGAAA; 11M-Gh-R2: GCTTCCAGG-AACAAGATTGACA; 11M-Gh-F3: TAAGAGATCTAGCCACAGGGA; 11M-Gh-R3: CACTGCTGTTGGGAAAAGAAAG; 11M-Gh-F5: TCCT-ACCCTTGGATTCAAAA; 11M-Gh-R5: ACCAGCTTGTGTCTCGTCA; 11M-Gh-F6: CCGTTTGTGGAAGCAGGAA; 11M-Gh-R6: ATAACCC-CAGGCTAGTCCAT; 11M-Gh-F8: GACAGTGCCCTCTAGTGCTCA-GTG; 11M-Gh-R8: TTATCGTCTCATCGCCACCTTTGC. These were set up in 25-μl PCRs carried out on 10 ng genomic DNA, using Pharmacia Taq-DNA polymerase (Amersham Pharmacia Biotech) for 28 amplification cycles consisting of 30 sec denaturation at 94 C, 30 sec annealing at 55 C, and 90 sec extension at 72 C. PCR amplicons were purified by using the QIAquick PCR purification kit (QIAGEN) according to the manufacturer's protocol. PCR products were sequenced using the PCR primer pair 11M-Gh-F2 and 11M-Gh-R2 and Big Dye thermal cycle sequencing kit (PE Applied Biosystems, PRISM). The reaction products were analyzed on an ABI 377 DNA sequencing device. Sequences were edited manually, and contingency assembly for mutation detection were performed using Sequencer version 4.0.5.

Genotyping

Because the *sma1* point mutation affects a restriction site for AVAII (New England Biolabs, Beverly, MA) a combined PCR and digestion strategy could be employed for identification of mutants. After DNA extraction from tail tip tissue (0.5–1 cm) according to http://www.jax.org/resources/documents/imr/protocols, a 621-bp fragment covering part of exon 4 and exon 5 of the GH gene was amplified using the primer pair 5'-TCG GAC CGT GTC TAT GAG AAA-3' (forward) and 5'-GCT TCC AGG AAC AAG ATT GAC A-3' (reverse) (MWG Biotech). For amplification, 40 cycles consisting of 60 sec denaturation at 94 C, 60 sec annealing at 55 C, and 180 sec extension at 72 C were performed in a final volume of 50 μl. Sixteen microliters of the 621-bp amplicon were digested with 10 U AVAII and the resulting fragments separated on a 1.5% agarose gel. All mice in the colony were genotyped using this strategy.

Breeding and housing conditions of studied animals

For phenotypic characterization at Marburg University, a breeding colony was established from four dwarf males of the C3HeB/FeJ back-

ground (N2 to the first ENU-derived dwarf) and eight nonrelated wild-type C3HeB/FeJ females. Mice were kept in a non-SPF animal facility on a 12-h light,12-h dark cycle (lights on 0600 h) at an ambient temperature of 23 ± 2 C and fed Altromin 1314 standard breeding chow (Lage, Germany) *ad libitum*. For breeding, males were usually maintained with two females for a maximum period of 6 wk. Males were separated from females as soon as pregnancy was assessed from weight gain in females. Breeding cages were inspected for newborns every day, and gestation duration was calculated from the time interval between first day in breeding pair and resulting offspring day of birth. Offspring were weaned at 21 d, individually marked, and housed in groups of two to four individuals of the same sex. Because the number of mice per cage can influence uncoupling protein (UCP)-1 content in brown adipose tissue (BAT) and thereby affect energy expenditure (21), mice were kept singly for 2 wk before metabolic experiments. All experiments were performed in accordance with the German animal welfare laws.

Body weight and length measurements

Body weight was determined from d 7 to d 84 every 7 ± 1 d. Furless juveniles were individually marked by different patterns of foot paintings (Edding) and later by fur cuts. In a separate group of mice, body length was assessed on d 56 ± 1 (wk 8) (nose to anus distance in millimeters, d = ± 1 mm). For this procedure, all mice were briefly anesthetized with Halothan (Fluothane, Zeneca, Plankstadt, Germany) and placed dorsally in an extended position next to a ruler.

Pituitary GH immunostaining

Pituitary glands were obtained from dissected animals, fixed in 4% buffered formalin, and embedded in Technovit 7100 resin (Heraeus Kulzer, Hanau, Germany). For immunofluorescence 1.5-μm sections were blocked with 2% normal goat serum and incubated with an anti-GH polyclonal rabbit antibody [mouse GH (mGH); Diagnostic International GmbH, Germany] for 1 h (dilution: 1:500 in 1% BSA) at room temperature. The secondary antibody, Alexa Fluor 568 goat antirabbit IgG (H+L) (Molecular Probes Inc., Eugene, OR), was incubated for 1 h (dilution: 1:250 in 2% normal mouse serum) at room temperature. Nuclei were stained for two min with 4',6-diamidino-2-phenylindole (Sigma, St. Louis, MO) and sections were covered with fluorescent mounting medium (Dako Corp., Carpinteria, CA). Pictures were taken by a Axiovision system (Carl Zeiss, Göttingen, Germany) using double-exposure technique and 750 ms time of exposure for detecting the GH-immunostaining signal. For Western blot analysis of pituitary GH, shock-frozen pituitaries were sonicated in 12 μl radioimmunoprecipitation assay buffer [50 mM Tris-HCl (pH 7.5); 150 mM NaCl; 1% Non-indet-P40; 0.25% sodium desoxycholate, 1 mM EDTA]. An aliquot of the homogenate (1 μl) was briefly boiled in sodium dodecyl sulfate (SDS) buffer [2% SDS, 60 mM Tris-HCl (pH 6.8), 10% glycerol, 5%-dithiothreitol, 0.01% bromphenole blue], fractionated in 15% SDS-PAGE, and transferred by semidry blotting to nitrocellulose membrane (HybondC; Amersham Pharmacia Biotech). Membranes were probed using a rabbit antirat-GH antibody (1:90,000), obtained through the National Hormone and Pituitary Program (Dr. A. F. Parlow, National Institute of Diabetes and Digestive and Kidney Diseases, Torrance, CA). Immunoreactive GH protein was detected by enhanced chemiluminescence (Super Signal, Pierce, IL).

Measurement of major urinary protein (MUP)

Urine was collected from unrestricted 3-month-old mice between 0800 and 0900 h and centrifuged briefly for 3 min at 8800 × *g*. Two microliters of the supernatant were loaded in SDS buffer as described above. Samples were fractionated in 12% SDS-PAGE and subsequently stained with Coomassie blue. MUP (~20 kDa) represents the major protein component of mouse urine. MUP expression requires pulsatile occupancy of liver GHRs, and adult males secrete more than 3 times as much MUP as do females (22).

Blood chemistry and organ preparations

For organ preparation, previously nonfasted mice were anesthetized with CO_2 and killed by bleeding of the vena cava inferior. Dissections

were always carried out between 0900 and 1200 Central European Time. Blood samples of 0.3–0.5 ml were collected from the thoracic cavity with a syringe rinsed in 100 mM EDTA, 0.9% NaCl (pH 7.0). The plasma concentrations of IGF-1 were determined by enzyme immunoassay (10–2900, Diagnostic Systems Laboratories Inc., Webster, TX), and leptin was determined using a commercially available ELISA (Crystal Chem Inc., Chicago, IL). Blood samples for GH and ghrelin analysis were taken by retroorbital puncture. Ghrelin levels were measured using a commercially available RIA (Phoenixpeptide, Belmont, CA), and GH determinations were performed with a commercially available ELISA (IBL-Hamburg GmbH, Hamburg, Germany) using a specific polyclonal rabbit-antirat GH antibody (intraassay variation $< 3.7\%$, interassay variation $< 7.1\%$, lower detection limit: 0.11 μIU/ml, no cross-reactivity with human chorionic gonadotropin or human PL). Organs were quickly removed and weighed, and interscapular BAT (iBAT) and pituitaries were frozen in liquid nitrogen for subsequent Northern or Western blotting analysis.

Body composition

Body fat content was determined by 16-h Soxhlet extraction of dried carcasses using chloroform as the extracting agent. Before carcass analysis, the gastrointestinal tract and brain were removed ($\sim$2–3 g/animal). Fat-free dry mass (FFDM) is dry carcass mass minus fat mass.

Food intake

Seven-day cumulative food intake was determined at an age of 2–3 and 5–6 months in single mice maintained in their home cage in the animal facility.

Analysis of UCP1 expression

Total RNA was isolated from iBAT by single-step acid guanidinium-phenol-chloroform extraction using TRIzol reagent (Invitrogen Life Technologies, Carlsbad, CA), and 10 μg RNA were separated by electrophoresis in a formaldehyde-agarose minigel. RNA was transferred to a Hybond-N membrane (Amersham Pharmacia Biotech) and hybridized with a 1.10-kb ^{32}P-labeled hamster UCP1 cDNA probe and a 1.14-kb ^{32}P-labeled β-actin probe for 24 h at 63 C as described previously (23). UCP1 and β-actin mRNA hybridization signals were quantified by PhosphorImager (Storm 860, Molecular Dynamics, Amersham Pharmacia Biotech). UCP1 signals were normalized by β-actin expression. UCP1 protein content in iBAT was determined by Western blot analysis as published previously (24).

Statistical analysis

Unless otherwise stated, all comparisons were performed on a parametric basis by one-way-ANOVA, using body weight as a cofactor as indicated (analysis of covariance), and the resulting estimations of effect size include the 95% confidence intervals. Subsequent multiple *post hoc* comparisons were adjusted according to the method by Bonferroni, and different superscript letters (a, b, c) in figures, tables, and text indicate significant differences between genotypes as revealed by these multiple *post hoc* comparisons. For analysis of growth curves, repeated-measurement ANOVA was employed. Correlation coefficients were calculated according to Pearson. All results were considered statistically significant at $P < 0.05$.
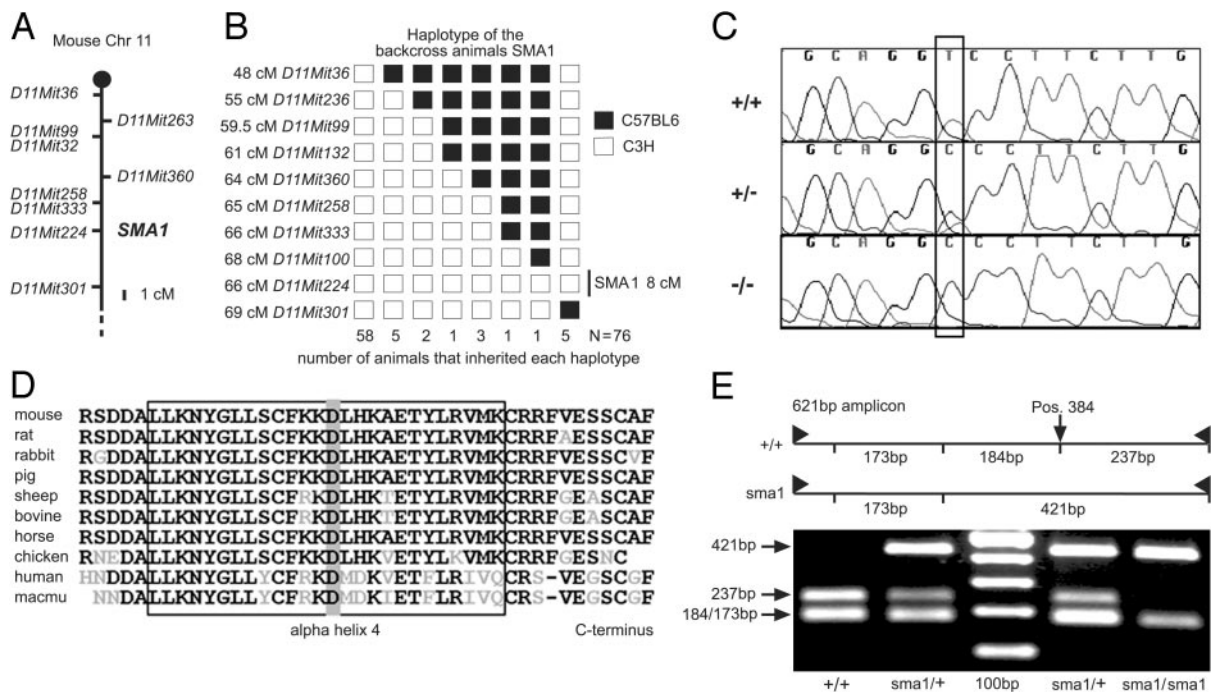

FIG. 1. Localization of the SMA1 mutation by intercross analysis and sequencing. A, The partial chromosome 11 linkage map shows the location of SMA1 in relation to a variety of relevant markers. B, Haplotype analysis for the SMA1 mutation on chromosome 11 in n = 76 [(C3HeB/FeJ-*sma1*/+ × C57BL/6Jico) × C56BL/6Jico mice] expressing a dwarf (SMA1) phenotype. The number of progeny that inherited each haplotype is given below the *boxes*. The frequency of recombination events places SMA1 in a region of approximately 8 cM between the microsatellite markers D11Mit333 and D11Mit301. C, Chromatograms resulting from sequencing part of exon 5 of the GH gene in C3HeB/FeJ-*sma1/sma1*, *sma1*/+, and +/+ mice. The chromatograms show the antisense strands from 3' to 5' end. Position 3144 of the nucleic acid sequence (GenBank accession no. Z46663) is highlighted in frame and reveals an a→g (5'→3') exchange in SMA1 mutants. D, Amino acid sequence alignment for GH across various vertebrate species. The *sma1*-mutation is located in the conserved fourth helix domain at the C terminus of the mature GH peptide, as indicated by the *box*. E, Genotyping of SMA1 mutants via AVAII restriction patterns of a 621-bp fragment amplified by PCR from exon 5 and part of exon 4 of the GH gene. In SMA1 mutants, the restriction site at position 384 of the PCR product is absent. Homozygous SMA1 are distinguished from heterozygous SMA1 by the 237-bp fragment from the wild-type allele. Fragments were separated on 1.5% agarose gels. The uninformative 173-bp and the 184-bp fragments are not resolved.

Results

Site and nature of the sma1 mutation

The analysis of 48 [(C3HeB/FeJ-*sma1*/+ × C57BL/6Jico) × C57BL/6Jico] mice revealed that the SMA1 phenotype cosegregates with the marker D11Mit224 on chromosome 11 (Fig. 1A). A more detailed haplotype analysis mapped the mutation between the microsatellite markers D11Mit333 and D11Mit301, a position in which the GH gene is located (Fig. 1B). The sequence analysis as shown by the chromatogram (Fig. 1C) revealed the presence of an a→g transition (position 3144 of the nucleic acid sequence, GenBank accession no. Z46663) in exon 5 of the GH gene of C3HeB/FeJ-SMA1 heterozygous and homozygous mutant animals. This transition translates into a D167G amino acid exchange in the C-terminal helix of the mature protein (D193G of the propeptide), a domain that is highly conserved throughout species (Fig. 1D). Using the combined PCR and digestion strategy, SMA1 mutants were identified by the presence of an additional 421-bp fragment, which results from elimination of the AVAII restriction site at position 384 of the 621-bp PCR amplicon. Heterozygous SMA1 mice show an additional 237-bp fragment from the wild-type allele (Fig. 1E).

Longitudinal growth is retarded in SMA1 mice

As depicted in Fig. 2, A and B, adult SMA1 animals are lighter due to smaller size and length, with heterozygous mice showing an intermediate phenotype. Mean body weight is not significantly different between +/+ and *sma1*/+ or *sma1*/*sma1* mice until wk 2 in males and wk 3 in females (Fig. 2C). However, within each litter containing *sma1*/*sma1* pups (n = 6 of 11 litters, three to five pups per litter), these were found to be the smallest individuals at 7 d of age.

With progressing age, the body weight differences between genotypes increase, resulting in a lower body weight of about 70% in *sma1*/+ mice and 50% in *sma1*/*sma1* mice, compared with +/+ littermates at 12 wk. As evident from the growth rates (Fig. 2D), the peripubertal growth spurt that usually occurs in wild-type mice at 3–4 wk is reduced in *sma1*/+ and absent in *sma1*/*sma1* animals. Beyond 6 wk of age, *sma1*/*sma1* mice show uniform longitudinal growth rates indistinguishable from +/+ and *sma1*/+ mice. Sexual dimorphism in weight and length is preserved in *sma1*/+ but not in *sma1*/*sma1* mice (Fig. 2B).

In accordance with reduced body weight and size, which persist for lifetime, SMA1 mice have reduced mean organ sizes (Fig. 3). In +/+ and *sma1*/+, all organ weights except brain weight display high correlation coefficients with body weight (+/+: $0.580 \leq r^2 \leq 0.935$; *sma1*/+: $0.708 \leq r^2 \leq 0.994$, all $P < 0.05$; testes weight in +/+ ($P = 0.17$); n = 6–7). Correlation coefficients are lower in *sma1*/*sma1* ($r^2 \leq 0.707$) and do not reach statistical significance, which may result from low sample size (n = 5). Liver mass in *sma1*/+ and *sma1*/*sma1* is nonproportionally reduced, *i.e.* lower than expected from the relationship of body mass and liver mass in wild-type mice ($P < 0.001$, 95% confidence interval: 0.3–0.6 g for mean analysis of covariance estimated difference of
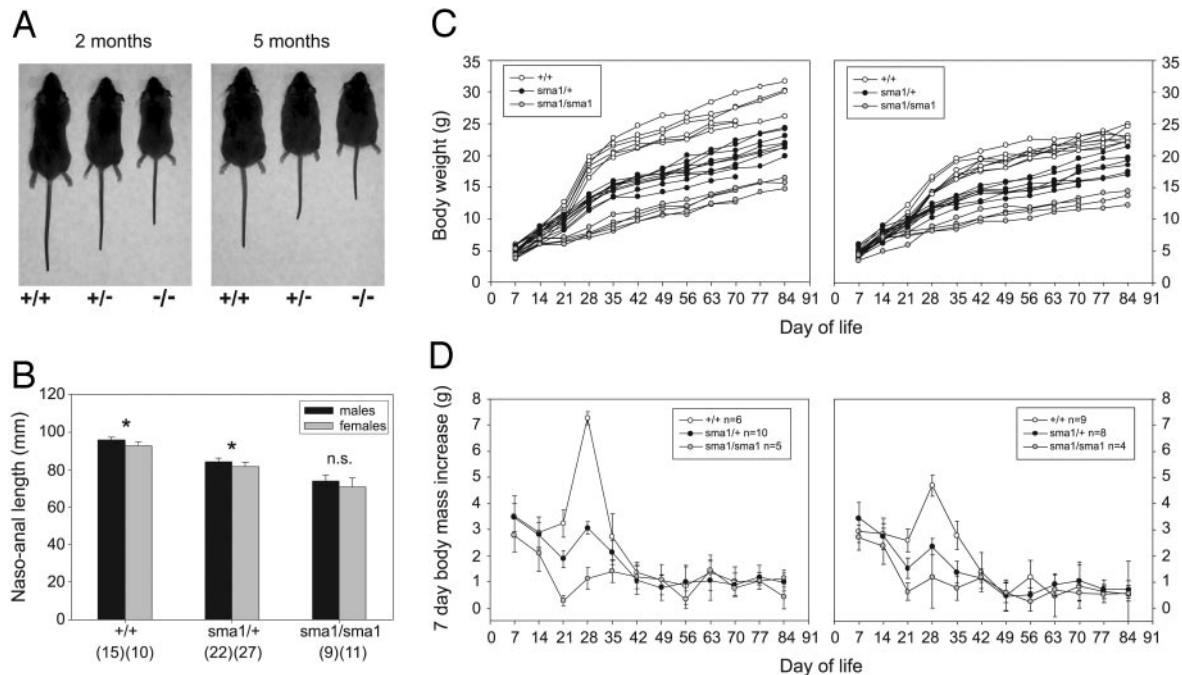

FIG. 2. A, Representative +/+, *sma1*/+, and *sma1*/*sma1* littermates at the age of 2 months and 5 months, respectively. B, Mean body length in SMA1 mutants is significantly decreased [$P < 0.001$, df = 5, F = 169.979; $P < 0.001$ (sex); $P = 0.75$ (genotype × sex)]. *Bars* depict mean ± SD; the number of mice included in each group is indicated in *brackets*. *, $P < 0.05$ (*t* test) for body length of males *vs.* females (*sma1*/*sma1*: $P = 0.1$). C, Growth curves of male (*left panel*) and female (*right panel*) +/+, *sma1*/+, and *sma1*/*sma1* mice from d 7 ± 1 to d 84 ± 1. D, Mean 7-d body mass increase (±SD) of the animals depicted in C. For calculation of the growth rate during the first week of life, a uniform birth weight of 1.5 g was assumed for each genotype and sex (*cf.* text).
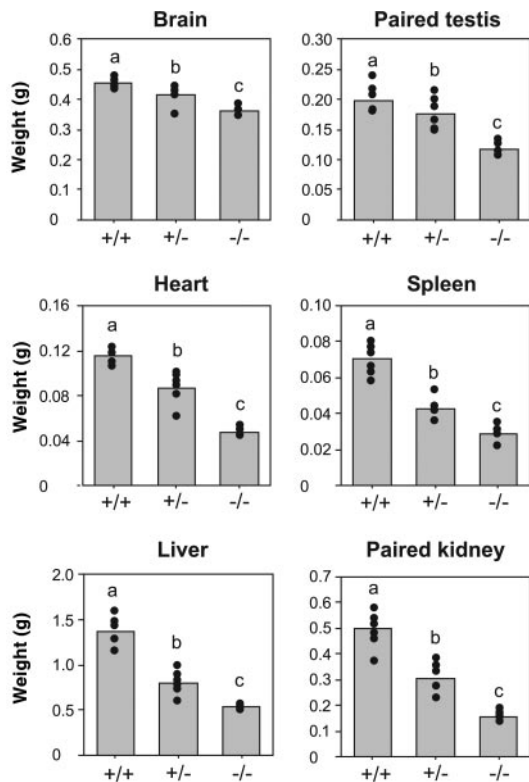
FIG. 3. Organ weights are significantly reduced in male SMA1 mice at the age of 2–3 months (a, b, c: $P < 0.05$). *Bars* indicate mean organ weights of n = 7 +/+, n = 6 *sma1*/+ and n = 5 *sma1/sma1* individuals (males only), and the *black symbols* show the distribution of data from individual mice.

liver weight between mutants of either genotype and +/+ at a body weight of 21.9 g). Except for their smaller size, all organs dissected did not exhibit gross anatomic abnormalities.

Viability and fertility of SMA1 mice

Sma1/+ and *sma1/sma1* mice are fertile and reproduce offspring. However, complete breeding failure (no surviving pups due to perinatal mortality of the entire litter) is significantly increased in [(*sma1*/+)♂ × (+/+)♀] (16%; $P = 0.002$; $\chi^2 = 12.457$) and *sma1/sma1* inbreeding (32%; $P \leq 0.001$; $\chi^2 = 33.401$), compared with [(+/+) × (+/+)] breeding pairs (5%). In contrast, postnatal mortality in single pups within a litter was observed in very few cases only, which in *sma1*/+ inbreeding did not selectively affect *sma1/sma1* animals. This indicates that offspring genotype had no effect on postnatal survival.

Median litter size at weaning (all pups surviving) is influenced by parental genotype combination, with lowest number of pups in *sma1/sma1* inbreeding and intermediate litter size in *sma1*/+ inbreeding (Table 1). Participation of either *sma1*/+ male or female in matings to +/+ does not affect median litter size. In contrast, maximal litter size is dependent on the female genotype, possibly reflecting maternal-fetal size mismatch or fetal undernutrition in mutants.

The frequency distribution of genotypes at weaning

TABLE 1. Litter size in SMA1 and wild-type mice with respect to different combinations of parental genotype

Cross-parental genotype (♂ × ♀)	n	Litter size		
		Min	Median	Max
(+/+) × (+/+)	20	3	6	10
(sma1/+) × (+/+)	30	3	6	9
(+/+) × (sma1/+)	6	3	5–6	7
(sma1/+) × (sma1/+)	31	1	4	6
(sma1/sma1) × (sma1/sma1)	13	2	3	4

n, Number of breeding pairs; Min, minimum; Max, maximum.

among surviving mice resulting from *sma1*/+ inbreeding and [(*sma1*/+)♂ × (+/+)♀] breeding, and the resulting distribution frequencies of phenotypes are in accordance with a semidominant Mendelian trait (Table 2). There is a bias against *sma1/sma1* offspring in heterozygous inbreeding, which may reflect increased pre- or perinatal mortality in these genotypes, but the deviance from 25% is not significant ($P = 0.21$; $\chi^2 = 3.081$; $df = 2$). The frequency distribution of each sex among genotypes is equal in all groups (data not shown).

Sexual maturation in *sma1/sma1* females is significantly delayed by approximately 1 wk, compared with +/+ and *sma1*/+ females, as assessed from timing of vaginal opening (median age *sma1/sma1*: 40d[a] (n = 9), +/+: 34d[b] (n = 11), and *sma1*/+: 31d[b] (n = 22), $P < 0.05$), but gestation is not affected (minimum 20 d; median 22–23 d for each genotype).

Pituitary architecture and GH immunostaining

The pituitary gland is reduced in overall size and weight in adult mutants at 3 months (median weight: +/+ 0.0015 g; *sma1*/+: 0.0010 g; *sma1/sma1*: 0.0006 g; n = 5–6 per genotype), and the anterior lobe is nonproportionally reduced in relation to the posterior lobe (Fig. 4, A–C). The acidophil cells of the anterior lobe, normally numerous and readily identified in control mice due to their strongly acidophil granules in cytoplasm, are nondetectable in the pituitaries of both *sma1*/+ and *sma1/sma1* mice (Fig. 4, D–F). By immunofluorescence (Fig. 4, G–I) we could detect strong GH immunostaining in wild-type mice but only traces of GH in *sma1*/+ and almost no GH immunostaining in pituitaries of *sma1/sma1*. Interestingly, the residual GH immunostaining in *sma1/sma1* appears to be related to single cells, with the majority of pituitary cells displaying almost no fluorescence at all. These graded results were confirmed by Western blot analysis of pituitary protein content, which showed greatly reduced pituitary GH in homozygous SMA1 and reduced GH immunostaining in heterozygous SMA1 (Fig. 5A).

IGF-1- but not GH-correlated dwarfism and hyperghrelinemia in SMA1 mice

Adult SMA1 mice have significantly lower plasma IGF-1 concentrations, which are correlated with body length across genotypes ($r^2 = 0.77$, $P < 0.001$), but the intermediate IGF-1 levels displayed by *sma1*/+ are reduced by more than 50% when compared with +/+ mice (Fig. 5C). Plasma GH was detected in two of eight *sma1*/+ individuals and was below the detection limit of the specific immunoassay used in all *sma1/sma1* mice. As a biological marker of intact GH secre-

TABLE 2. Frequency distribution of offspring genotypes and phenotypes with respect to different parental genotype combinations

Cross-parental genotype (♂ × ♀)	n	Genotype level				Phenotype level		
		Offspring genotype	Observed (%)	Expected (%)	P (χ^2 test)	Offspring phenotype	Sensitivity (%)	Specificity (%)
(sma1/+) × (+/+)	36 (186)	+/+	47.3	50.0	0.46	Wild-type		99.8
		sma1/+	52.7	50.0		Dwarf	92.8	
(+/+) × (sma1/+)	6 (31)	+/+	48.4	50.0	0.86	Wild-type		100
		sma1/+	51.6	50.0		Dwarf	100	
(sma1/+) × (sma1/+)	37 (149)	+/+	29.5	25.0	0.21	Wild-type		100
		sma1/+	51.0	50.0		Dwarf	98.0	
		sma1/sma1	19.5	25.0				

For phenotyping SMA1, a threshold body weight of at least 18.4 g (males) and at least 15.0 g (females) on d 41–43 was established according to Ref. 19. This procedure yields an overall sensitivity of 95.8% (SMA1) and a specificity of 99% (WT) in predicting mutants from body weight on d 41–43. n, Number of breeding pairs. Number of individuals is in *parentheses*. Dwarf phenotypes obtained from *sma*1/+ inbreeding show a clear bimodal weight distribution pattern that correlates with genotype, indicating semidominance of the trait.
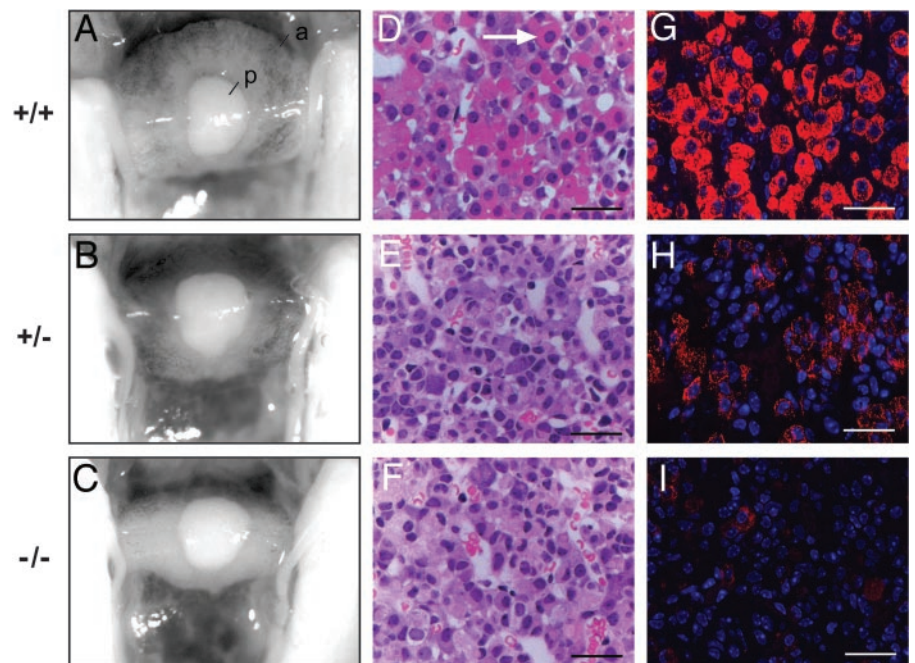
FIG. 4. A–C, Dorsal view on the pituitary gland. The anterior lobe (a) is nonproportionally reduced in SMA1 in relation to the posterior lobe (p). D–F, Hematoxylin-eosin cross-sections of the anterior pituitary lobe (×400). A typical mature somatotroph cell in a wild-type animal is marked by the *arrow*. (G–I). Representative anti-mGH immunostaining of the anterior pituitary lobe (resin sections; ×400). *Scale bars*, 50 μm.

tion, we investigated urinary MUP levels in male and female mice aged 3 months (Fig. 5B). MUP expression is lower in *sma*1/+ and below the detection limit in *sma*1/*sma*1 mice of either sex. Despite reduced MUP excretion in *sma*1/+ mice, the sexually dimorphic pattern of urinary MUP excretion is preserved in this genotype, suggesting intact GH secretion pattern from the pituitary gland. Plasma ghrelin levels in mice aged 2–3 months are significantly higher in *sma*1/*sma*1 mice when compared with +/+ mice, with *sma*1/+ mice showing intermediate levels, without significantly differing from either +/+ or *sma*1/*sma*1.

SMA1 are small and mice become obese

As expected from the dwarf phenotype, the FFDM of SMA1 is significantly reduced, with more than 50% of the reduction already observed in heterozygous mice (Table 3). The FFDM of the examined mice is significantly correlated with body weight in all genotypes at 2–3 months and 5–6 months, respectively (all $P < 0.001$, $0.800 \leq r^2 \leq 0.987$, except *sma*1/*sma*1 at 5–6 months: $P = 0.112$, $r^2 = 0.256$). The re-

duction in FFDM of SMA1 is nonproportional with body weight (see the supplemental figure, A and B, published on The Endocrine Society's Journals Online Web site at http://endo.endojournals.org), suggesting altered body composition in mutants.

Fat mass is also highly correlated with body mass in all groups of mutant and wild-type mice (all $P < 0.001$; $0.810 \leq r^2 \leq 0.990$), after strong linear and parallel relationships, which allow reliable estimations of individual body fat content in mice aged 2–5 months simply by weighing a mouse (see the supplemental figure, C and D, and the supplemental table). Clearly, total fat mass is overproportionally enlarged in mutants, and percentage body fat can amount up to 46% of total body mass in some *sma*1/*sma*1 mice at 5–6 months (Table 3). Mean total body fat in the groups of mice investigated is not significantly different between wild-type and SMA1 mice at 5–6 months and also at 2–3 months, respectively. However, at 2–3 months, the latter finding reflects the impact of one particularly heavy individual in the *sma*1/*sma*1 group at 2–3 months (19.9 g body weight, 8.3 g body fat),
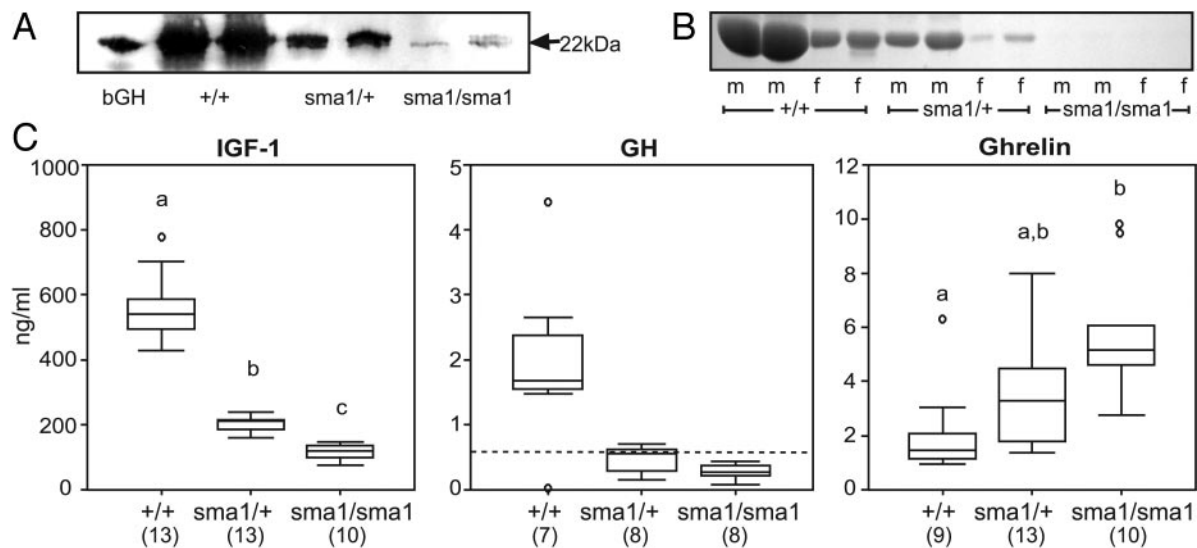
FIG. 5. A, Immunological detection of pituitary GH content in mice aged 3 months. The reduction in total GH protein content is greater than expected from reduced pituitary size (*sma1/+*: 32%, *sma1/sma1*: 4% of wild-type GH immunostaining, as assessed densitometrically). B, Urinary MUP (~20 kDa) excretion in male (m) and female (f) wild-type and SMA1 mice at 3 months. C, IGF-1, GH, and ghrelin plasma levels in wild-type and SMA1 mice at the age of 2–3 months. Box plots indicate 50%, 25%, and 75% percentiles, respectively; whiskers show minimum-maximum. Outliers are indicated by *circles* according to SPSS software (SPSS Inc., Chicago, IL). The *sma1/sma1* group for IGF-1 determinations includes six mice at an age of 5–6 months (not significantly different from 2–3 months). In *brackets*, number of individuals, a, b, c: $P < 0.05$. Note that $P = 0.06$ for *sma1/+ vs. sma1/sma1* plasma ghrelin. For GH, the *dotted line* at 0.63 ng/ml equals the lower GH ELISA detection limit.

TABLE 3. Mean FFDM (fat-free-dry-mass), fat mass, and percentage body fat content [±SD, and range (min–max)] in wild-type and SMA1 mutants at 2–3 and 5–6 months, respectively

	2–3 months			5–6 months		
	+/+ (14)	sma1/+ (11)	sma1/sma1 (11)	+/+ (12)	sma1/+ (15)	sma1/sma1 (11)
Live body weight (g)	27.5 ± 3.6^a (22.0–34.9)	18.9 ± 2.8^b (15.4–24.2)	12.2 ± 2.8^c (9.2–19.9)	30.7 ± 3.8^a (24.3–36.3)	20.9 ± 4.9^b (13.2–30.0)	17.5 ± 3.7^c (12.7–24.3)
FFDM (g)	5.3 ± 0.7^a (4.2–6.5)	2.5 ± 0.4^b (2.0–3.2)	1.8 ± 0.2^c (1.5–2.4)	6.5 ± 0.7^a (5.4–7.7)	3.5 ± 0.6^b (2.4–4.9)	2.1 ± 0.4^c (1.6–2.8)
Fat mass (g)	3.6 ± 1.6^a (1.7–7.7)	4.1 ± 1.8^a (2.3–7.4)	2.8 ± 1.9^a (1.1–8.3)	5.0 ± 2.1^a (1.4–8.2)	5.9 ± 3.1^a (1.9–11.9)	6.2 ± 2.7^a (3.0–11.2)
% body fat	12.9 ± 3.8^a (7.2–22.2)	21.6 ± 5.8^b (14.9–30.5)	21.2 ± 7.5^b (12.4–41.6)	15.8 ± 5.4^a (5.6–22.9)	26.5 ± 8.5^b (14.1–39.8)	34.2 ± 7.9^c (21.4–46.2)

Number of individuals is in *parentheses*. *Superscripts* refer to multiple comparisons between genotypes within each age group (^{a,b,c}, $P < 0.05$).

which biases body fat content toward a higher mean value. Body fat is significantly lower in *sma1/sma1* at 2–3 months (*i.e.* 2.2 ± 0.6 g) if this individual is excluded from the statistical analysis as an outlier.

An analysis of body fat distribution by determining selected fat depot weights in an additional group of male mice demonstrates that obesity is predominantly due to a non-proportional enlargement of the posterior subcutaneous depot (combined inguinal and dorsolumbar pads) (Table 4). The volumes of site-specific fat depots are all strongly correlated with body weight ($0.733 \leq r^2 \leq 0.670$; all $P < 0.001$; $n = 10–12$), and the nonproportional increase observed in total body fat of mutants is reflected in each fat depot (data not shown).

In summary, body fat in adult SMA1 is higher than expected in relation to their reduced body size, with mutants at 5–6 months appearing to accumulate almost equal amounts of total white adipose tissue in a significantly smaller body, preferably in the posterior sc region. At 2–3

months, obesity is less pronounced in *sma1/sma1* mice when compared with *sma1/+* mice, and concomitantly mean plasma leptin levels in +/+ and *sma1/+* mice are similar in mice aged 2–3 months [+/+: 3.0 ± 0.7 ng/ml (n = 13), *sma1/+*: 3.5 ± 0.6 ng/ml (n = 12)], and slightly lower in *sma1/sma1* [2.3 ± 0.4 ng/ml (n = 3)]. In *sma1/sma1* aged 5–6 months, plasma leptin levels increase to 9.5 ± 4.9 ng/ml (n = 6), in accordance with increasing adiposity. Across genotypes, plasma leptin concentrations significantly correlate with fat mass ($P < 0.001$, $r^2 = 0.88$), and the relationships between body fat and leptin levels of each genotype are within the same line of regression, supporting that in SMA1 leptin simply reflects body fat content regardless of genotype.

In accordance with white adipose tissue depot weights, mean iBAT weight is not significantly different between genotypes in younger mice, and it is lower in older SMA1 mice (Table 4). When viewed from a weight-adjusted approach, however, iBAT is nonproportionally enlarged in mutants of

TABLE 4. Dissected adipose tissue (AT) weights of male wild-type and SMA1 mutants at 2–3 and 5–6 months

	2–3 months			5–6 months		
	+/+ (7)	sma1/+ (6)	sma1/sma1 (5)	+/+ (5)	sma1/+ (6)	sma1/sma1 (5)
BW (g)	25.9 ± 2.5^a	18.1 ± 3.0^b	11.6 ± 1.8^c	36.3 ± 5.5^a	21.3 ± 3.6^b	17.2 ± 1.9^c
IAT (g)	0.467 ± 0.160^a	0.593 ± 0.189^a	0.545 ± 0.253^a	1.370 ± 0.241^a	1.336 ± 0.542^a	1.410 ± 0.235^a
EAT (g)	0.328 ± 0.131^a	0.333 ± 0.161^a	0.143 ± 0.067^a	1.186 ± 0.361^a	0.732 ± 0.341^b	0.493 ± 0.151^b
MAT (g)	0.405 ± 0.112^a	0.388 ± 0.100^a	0.227 ± 0.071^b	0.849 ± 0.214^a	0.466 ± 0.130^b	0.372 ± 0.097^b
PAT (g)	0.121 ± 0.048^a	0.135 ± 0.070^a	0.060 ± 0.027^a	0.414 ± 0.136^a	0.253 ± 0.120^b	0.186 ± 0.062^b
iBAT (g)	0.061 ± 0.012^a	0.070 ± 0.017^a	0.055 ± 0.015^a	0.117 ± 0.020^a	0.079 ± 0.020^b	0.087 ± 0.013^b

The number of animals in each group is indicated in *parentheses. Superscripts* refer to multiple comparisons between genotypes within each age group (^{a,b,c}, $P < 0.05$). Numbers indicate mean ± SD. BW, Body weight; IAT, combined inguinal and dorsolumbar; EAT, epididymal; MAT, mesenteric; PAT, perirenal; iBAT, interscapular BAT.
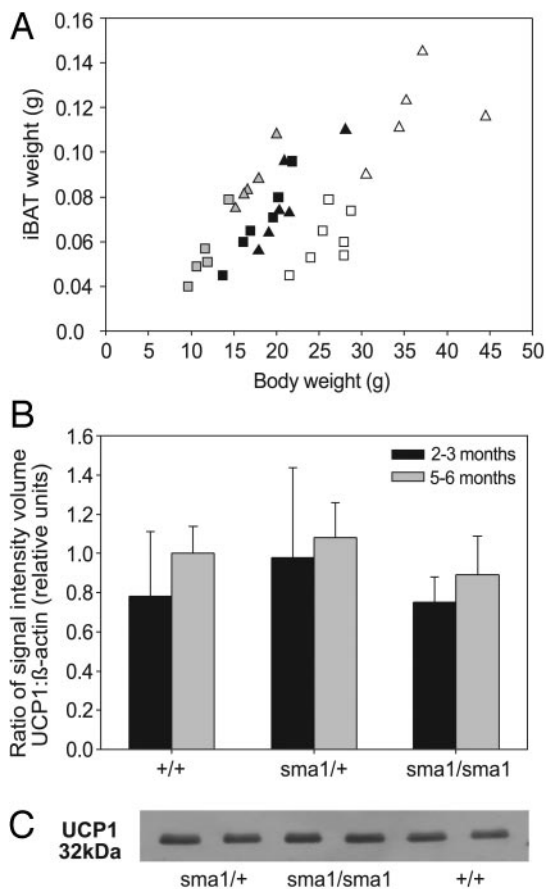
FIG. 6. A, Relationship between body weight and iBAT pad weight. *White symbols,* +/+; *black symbols, sma1/+; gray symbols, sma1/sma1. Squares,* mice aged 2–3 months; *triangles,* 5–6 months. B, UCP1 mRNA expression in iBAT of wild-type and SMA1 mice at 2–3 and 5–6 months, respectively. *Bar,* Mean ± SD expression levels in relation to wild-type expression at 5–6 months (n = 5–7 mice in each group). C, Immunological detection of UCP-1 in iBAT of wild-type and SMA1 mice at 5 months. Each lane contained 20 μg total iBAT protein.

both age classes (Fig. 6A). Total RNA from iBAT yielded 1.3 ± 0.3 μg/mg (+/+), 1.3 ± 0.4 μg/mg (sma1/+), and 1.3 ± 0.2 μg/mg (sma1/sma1) at 2–3 months and 0.9 ± 0.2 μg/mg (+/+), 1.3 ± 0.2 μg/mg (sma1/+), and 1.0 ± 0.2 μg/mg (sma1/sma1) at 5–6 months, respectively ($P = 0.38$ (genotype); $P = 0.01$ (age); $P = 0.27$ (genotype × age); ANOVA $P = 0.08$; $df = 5$; F = 2.26). UCP-1 expression is not altered in iBAT of SMA1 mice as revealed by Northern blot and Western blot analysis (Fig. 6, B and C).

The accumulation of body fat in SMA1 is not accompanied by excessive daily food intake at 2–3 months (+/+: 4.2 ± 0.4 g^a (n = 13); sma1/+: 2.9 ± 0.3 g^b (n = 17); sma1/sma1: 2.4 ± 0.3 g^c (n = 14); $P < 0.05$, *i.e.* food intake in sma1/+ and sma1/sma1 mice reflects lower body size. At 5–6 months, larger +/+ mice (31.6 ± 4.7 g) consume significantly more food [+/+: 3.6 ± 0.5 g^a (n = 23)] than SMA1 mice, but at this age mean food intake is not different in sma1/sma1 mice, compared with sma1/+ mice [sma1/+: 2.6 ± 0.4 g^b (n = 21); sma1/sma1: 2.5 ± 0.5 g^b (n = 17); $P < 0.05$] despite lower body weight in the latter group (sma1/+: 21.0 ± 3.5 g; sma1/sma1: 16.1 ± 2.0 g).

Other phenotypic observations

Over all, sma1/+ and sma1/sma1 appear healthy and vigorous, but there is a clear delay in maturation and the development in the homozygous SMA1 phenotype. Up to 3 months of age, sma/sma1 individuals appear pedomorphic and resemble +/+ weanlings, both in appearance and behavior (*i.e.* characteristic vigorous tail shaking when anxious). Fur cuts, applied as individual tags, remained visible for a longer period in sma1/sma1 mice, compared with +/+ and sma1/+ mice. Similarly, disproportional accumulation of body fat is already visible at 3 months, but sma1/sma1 mice catch up with +/+ and sma1/+ with respect to their total body fat, thereby dramatically increasing percentage body fat.

Discussion

In humans and animals, syndromes of heritable dwarfism can be caused by states of GH resistance or GH deficiency, with either dominant or recessive inheritance, some of which are related to point mutations. Using random ENU-mutagenesis, we created a novel mouse model for dwarfism due to a missense mutation in the GH gene, which displays some unique phenotypic features already evident at this early stage of investigation. We show that the SMA1 mutation leads to a genotype-dependent growth deficiency; in fact, the SMA1 mouse represents the first nontransgenic animal model to exhibit heritable dwarfism in a semidominant Mendelian pattern. The phenotypic differences in body size manifest during puberty, but an effect of genotype on body weight appears to be already present in juveniles as early as 1 wk of age. Additional measurements of individual new-

born *sma1/sma1* yielded body weights of 1.2–1.6 g, comparable with +/+ inbreeding offspring (1.1–1.6 g) from similar litter sizes, indicating that either birth weight is not altered or a high number of litters is needed for detecting statistically significant differences between genotypes in weight of newborns.

The reduction in size of SMA1 appears to be promoted predominantly by the inability of the mutated GH to stimulate postnatal growth either directly or indirectly via circulating IGF-1 levels, which are gradually reduced as a consequence of genotype heterocygotic or homocygotic for the GH point mutation. During puberty, increasing circulating IGF-1 has been demonstrated to be directly related to the peripubertal GH spurt, in line with its predominant role in bone formation and lean mass increase (25). Surprisingly, in mice aged 2–3 months, our measurements demonstrate low to undetectable plasma GH levels in both *sma1/+* and *sma1/sma1*, suggesting both genotypes to be peripherally GH deficient at this age. However, because GH is released from the pituitary in an ultradian, pulsatile pattern (26), failure to detect GH in a single plasma specimen does not necessarily indicate absence of GH secretion. Indeed, the genotypic gradations seen in IGF-1 production, and persistence of the dimorphic pattern of urinary MUP excretion in *sma1/+*, compared with *sma1/sma1* individuals, support reduced, albeit intact, secretion pattern of GH in *sma1/+* but not *sma1/sma1* (22).

As judged from spontaneous dwarf rats, *dr/dr* rats , which do not produce GH due to abnormal mRNA splicing, expression of one intact allele is sufficient to support normal growth in heterozygous individuals (27). Similarly, growth failure in humans and rodents caused by GH deficiency due to impaired responsiveness of pituitary somatotrophs to GHRH (28, 29) as well as in states of GH resistance or insensitivity (Laron syndrome), expression of one allele can support normal growth in the heterozygous genotype (30–32). Contrasting these observations, in SMA1 one intact allele is clearly not sufficient for restoring the wild-type phenotype. It remains to be elucidated how a GH gene dosage effect could be translated into a dominant GH reduction, giving rise to a semidominant, IGF-1-dependent phenotype. The finding that in heterozygous SMA1 both FFDM and IGF-1 levels are more than 50% reduced, compared with wild-type mice, already suggests that the SMA1 phenotype is caused by more complex growth interference than expected from a simple GH-gene dosage relationship.

In the absence of significant amounts of immunodetectable GH in the blood of heterozygous mice, there is intermediate to subintermediate GH immunostaining in anterior pituitary and GH immunostaining in residual cells of *sma1/sma1*. The graded result of pituitary GH immunoreactivity was confirmed by Western blot analysis, and total pituitary GH content is dramatically reduced as the number of somatotroph cells decreases. The combined findings therefore strongly suggest both impairment in pituitary GH storage, possibly due to reduced number of somatotroph cells, and impaired GH secretion in SMA1 mice.

In humans, clinical syndromes associated with reduced or absent GH expression and a deficiency in IGF-1 can be inherited as an autosomal recessive (isolated GH deficiency-1)

or an autosomal dominant (isolated GH deficiency-II) trait (33–35). The latter have been hypothesized to result from mutant allele products that interfere with normal storage or secretion of the wild-type-protein (36, 37). In fact, only recently McGuinness *et al.* (38) reported that one of the GH gene splice variants, Δ^{exon3}human GH (hGH), generates a 17.5-kDa hGH that lacks amino acids 32–71 and can exert a dominant-negative effect on wild-type-hGH production both *in vitro* and *in vivo*. The dominant-negative Δ^{exon3}hGH has been shown to inhibit wild-type-hGH secretion in a concentration-dependent manner (39), and the anterior pituitaries of Δ^{exon3}hGH-transgenic mice showed marked hypoplasia and a profound reduction in cells staining for GH by immunohistochemistry.

Based on our phenotypic analysis of SMA1, we propose the structure of the mature *sma1*-GH to be altered, thereby preventing correct folding, storage, or secretion and hence signaling due to deleterious folding of the GH molecule at the level of the somtatotrophic pituitary cell. Support for this hypothesis derives from crystal structure analysis of the hGH molecule (40), which shares 62% sequence identity (73% similarity) with mouse GH (mGH). The inspection of hGH D169 (positional homologue to mGH D167) reveals that the residue is directed to the core of the protein with each side chain oxygen atom being involved in intramolecular hydrogen bonds. The Oδ1 of D169 forms a hydrogen bond to Oγ of S55 as well as to Nϵ1 of W86. A weaker hydrophobic interaction connects Oδ2 of D169 and Nζ of K172. Given the perfect conservation at the homologous position of S55, W86, and D169 in all published GH sequences, this observation strongly points to stabilizing role of D169, an assumption that also fits well with the poor expression rate of both a human D169A mutant (41) and the murine SMA1 D167G variants in *Escherichia coli* (Wolf S. and G. Franke, Ingenium Pharmaceuticals, personal communication).

The fact that single immunopositive cells are visible in *sma1/sma1* pituitaries is in agreement with a temporal and/or spatial degradation process, which may take place in somatotroph subpopulations of the pituitary and ultimately cause hypoplasia of the anterior lobe. Transgenic mice expressing thymidine kinase and acquiring pharmacological sensitivity to synthetic nucleosides (42), or transgenics expressing diphtheria toxin A genes under the control of the GH promoter (43), have demonstrated the existence of a common somatomammotroph stem cell precursor, which expresses GH and prolactin and has the capacity for self-regeneration. This population of self renewing cells is present in spatially distinct proliferative zones of the pituitary (44), and its mitotic activity may account for continuous residual GH immunostaining in *sma1/sma1* mice before subsequent degradation.

However, *in vitro* studies of bovine GH (bGH) variants have also demonstrated the importance of the residues encoded by exon IV and also exon V (mGH residues 125–190) for proper sorting of the GH protein to the secretory granules (45). Furthermore, dwarfism via impaired GH signaling has also been induced by functional antagonism due to overexpression of a mutated bGH analog (bGH119K) (46). In these transgenic mice, the degree of growth suppression was correlated with serum levels of bGH analog, and IGF-1 levels

were markedly reduced (47). At the present state of phenotypic analysis of SMA1, dominant-negative action of *sma1*-GH, possibly driven by increased hypothalamic releasing activity via ghrelin and other GH secretagogues, and its increasing interference with residual wild-type GH is the most favorable hypothesis that we can presently put forward to explain the semidominant, IGF-correlated phenotype, which is unique among models of heritable dwarfism and IGHD syndrome in man (34). Further research on SMA1 is required to fully understand all mechanisms involved in the generation of the semidominant phenotype.

Obesity is frequently associated with impairments of the GH axis in rodents as well as humans, and the finding that SMA1 mice become obese certainly appears to be in agreement with the reduction or lack of lipolytic activity caused by reduced or absent biofunctional GH levels in heterozygous or homozygous SMA1 mice, respectively. In *lit /lit* mice, a model for isolated GH deficiency, obesity is evident starting from puberty (2). Transgenic mice developed by Kopchick and coworkers (48), which express a functional GHR antagonist (bGHG119K), display obesity of a similar magnitude (20% at 2–3 months) when compared with *sma1/sma1* mice, and are of similar size and weight. Very recently GHR/BP-KO mice have been reported to exhibit increased adipose tissue mass as well (49).

From a thermoregulatory perspective, we would expect small mice (*i.e. sma1/+* and *sma1/sma1*) to be confronted with higher thermogenic demands due to a relatively larger surface area compared with +/+ mice, thereby counteracting obesity. In small mammals, BAT represents the major source of nonshivering thermogenesis, *i.e.* heat generated by uncoupling the respiratory chain from ATP-synthesis via UCP1 (50, 51). The recruitment of BAT thermogenic capacity not only involves UCP1 synthesis but also increased mitochondrial biogenesis and proliferation of tissue mass (52). In agreement, Li *et al.* (49) have reported increased mRNA levels of UCP-1 in BAT of GHR/BP KO and bGHG119K mice and reduced levels in giant mice overexpressing bGH, suggesting GH to negatively regulate UCP1-expression. In contrast, in the present study the GH deficiency in SMA1 had no effect on UCP1 mRNA and protein levels, even though iBAT was nonproportionally enlarged. Because the nonproportional increase of tissue mass was not accompanied by increased UCP1 synthesis, and RNA content per milligram tissue was similar in all genotypes, the effect of genotype on iBAT mass is most likely related to increased triglyceride storage rather than increased thermogenic capacity *per se*. Further investigation on nonshivering thermogenesis, body temperature, and energy balance will be necessary to resolve the metabolic phenotypes in SMA1 and other obese dwarf models.

In addition to its GH-releasing ability, ghrelin may be one endocrine player in the promotion of elevated body fat content in SMA1 because it has been shown to potently stimulate food intake and reduce fat oxidation, thereby inducing obesity in rodents. However, with the exception of patients with Prader-Willi syndrome, ghrelin secretion patterns are generally markedly reduced in obese compared with normal-weight rodents and humans (53, 54). Furthermore, ghrelin is not elevated in GH-deficient dwarf rats but is in hypophy-

sectomized rats (15), which suffer from multiple endocrine deficiencies. In accordance with these findings, a marked increase in plasma ghrelin of hypothyroid rats, but reduced levels in the same model of GH-deficient dwarf rats has been reported in a different study (55). At present, to our knowledge SMA1 is the only published obese animal model exhibiting hyperghrelinemia, and thus SMA1 could provide an attractive research tool to further investigate the interactions between growth and energy homeostasis as well as for the screening and testing of novel ghrelin receptor antagonists, which are currently under development in numerous academic and for-profit laboratories. However, because GH deficiency in SMA1 will almost certainly affect other GH-dependent pathways such as lipoprotein lipase activity, glucose uptake, and food intake (56), the amount of body fat observed in SMA1 and other GH-deficient rodents and subjects is also likely to reflect the lack of additional direct metabolic actions of GH. With respect to possible altered energy partitioning in SMA1, we hypothesize that in heterozygous SMA1 earlier onset of excessive nonproportional fat accumulation may be promoted by combined effects of elevated ghrelin levels, reduced directly GH-dependent lipolytic activity, and increased caloric intake or feed/gain efficiency.

In summary, we conclude that that the D167G mutation in the SMA1 mouse GH leads to a variant protein that most probably exerts the majority of its effects through disturbance of postnatal growth via some yet unknown mechanism that affects pituitary GH storage and release. The semidominant phenotype of SMA1 is unique among dwarf rodent models and will provide new insights into the mechanisms of GH/IGF-1-mediated growth. Furthermore, SMA1 mice are obese and display elevated ghrelin levels, thereby linking the metabolic and the growth axis in a unique semidominant way, which could establish SMA1 a suitable research tool for the investigation of future roles for ghrelin receptor agonists and antagonists in the regulation of energy balance and nutrient partitioning.

References

1. **Kopchick JJ, Andry JM** 2000 Growth hormone (GH), GH receptor, and signal transduction. Mol Genet Metab 71:293–314
2. **Donahue LR, Beamer WG** 1993 Growth hormone deficiency in 'little' mice results in aberrant body composition, reduced insulin-like growth factor-I and insulin-like growth factor-binding protein-3 (IGFBP-3), but does not affect IGFBP-2, -1 or -4. J Endocrinol 136:91–104
3. **Furuhata Y, Kagaya R, Hirabayashi K, Ikeda A, Chang KT, Nishihara M, Takahashi M** 2000 Development of obesity in transgenic rats with low circulating growth hormone levels: involvement of leptin resistance. Eur J Endocrinol 143:535–541

4. **Roemmich JN, Huerta MG, Sundaresan SM, Rogol AD** 2001 Alterations in body composition and fat distribution in growth hormone-deficient prepubertal children during growth hormone therapy. Metabolism 50:537–547

5. **Le Roith D, Scavo L, Butler A** 2001 What is the role of circulating IGF-I? Trends Endocrinol Metab 12:48–52

6. **Berelowitz M, Szabo M, Frohman LA, Firestone S, Chu L, Hintz RL** 1981 Somatomedin-C mediates growth hormone-negative feedback by effects on both the hypothalamus and the pituitary. Science 212:1279–1281

7. **Tannenbaum GS, Guyda HJ, Posner BI** 1983 Insulin-like growth factors: a role in growth hormone-negative feedback and body weight regulation via brain. Science 220:77–79

8. **Wallenius K, Sjogren K, Peng XD, Park S, Wallenius V, Liu JL, Umaerus M, Wennbo H, Isaksson O, Frohman L, Kineman R, Ohlsson C, Jansson JO** 2001 Liver-derived IGF-I regulates GH secretion at the pituitary level in mice. Endocrinology 142:4762–4770

9. **Butler A, Le Roith D** 2001 Control of growth by the somatotropic axis: growth hormone and the insulin-like growth factors have related and-independent roles. Annu Rev Physiol 63:141–164

10. **Lupu F, Terwilliger JD, Lee K, Segre GV, Efstratiadis A** 2001 Roles of growth hormone and insulin-like growth factor 1 in mouse postnatal growth. Dev Biol 229:141–162

11. **Kojima M, Hosoda H, Date Y, Nakazato M, Matsuo H, Kangawa K** 1999 Ghrelin is a growth-hormone-releasing acylated peptide from stomach. Nature 402:656–660

12. **Date Y, Nakazato M, Hashiguchi S, Dezaki K, Mondal MS, Hosoda H, Kojima M, Kangawa K, Arima T, Matsuo H, Yada T, Matsukura S** 2002 Ghrelin is present in pancreatic α-cells of humans and rats and stimulates insulin secretion. Diabetes 51:124–129

13. **Tschop M, Smiley DL, Heiman ML** 2000 Ghrelin induces adiposity in rodents. Nature 407:908–913

14. **Wren AM, Small CJ, Abbott CR, Dhillo WS, Seal LJ, Cohen MA, Batterham RL, Taheri S, Stanley SA, Ghatei MA, Bloom SR** 2001 Ghrelin causes hyperphagia and obesity in rats. Diabetes 50:2540–2547

15. **Tschop M, Flora DB, Mayer JP, Heiman ML** 2002 Hypophysectomy prevents ghrelin-induced adiposity and increases gastric ghrelin secretion in rats. Obes Res 10:991–999

16. **Hrabe de Angelis MH, Flaswinkel H, Fuchs H, Rathkolb B, Soewarto D, Marschall S, Heffner S, Pargent W, Wuensch K, Jung M, Reis A, Richter T, Alessandrini F, Jakob T, Fuchs E, Kolb H, Kremmer E, Schaeble K, Rollinski B, Roscher A, Peters C, Meitinger T, Strom T, Steckler T, Holsboer F, Klopstock T, Gekeler F, Schindewolf C, Jung T, Avraham K, Behrendt H, Ring J, Zimmer A, Schughart K, Pfeffer K, Wolf E, Balling R** 2000 Genome-wide, large-scale production of mutant mice by ENU mutagenesis. Nat Genet 25:444–447

17. **Soewarto D, Fella C, Teubner A, Rathkolb B, Pargent W, Heffner S, Marschall S, Wolf E, Balling R, Hrabe DA** 2000 The large-scale Munich ENU-mouse-mutagenesis screen. Mamm Genome 11:507–510

18. **Ehling UH, Charles DJ, Favor J, Graw J, Kratochvilova J, Neuhauser-Klaus A, Pretsch W** 1985 Induction of gene mutations in mice: the multiple endpoint approach. Mutat Res 150:393–401

19. **Fuchs H, Schughart K, Wolf E, Balling R, Hrabe DA** 2000 Screening for dysmorphological abnormalities—a powerful tool to isolate new mouse mutants. Mamm Genome 11:528–530

20. **Schalkwyk LC, Jung M, Daser A, Weiher M, Walter J, Himmelbauer H, Lehrach H** 1999 Panel of microsatellite markers for whole-genome scans and radiation hybrid mapping and a mouse family tree. Genome Res 9:878–887

21. **Himms-Hagen J, Villemure C** 1992 Number of mice per cage influences uncoupling protein content of brown adipose tissue. Proc Soc Exp Biol Med 200:502–506

22. **Norstedt G, Palmiter R** 1984 Secretory rhythm of growth hormone regulates sexual differentiation of mouse liver. Cell 36:805–812

23. **von Praun C, Burkert M, Gessner M, Klingenspor M** 2001 Tissue-specific expression and cold-induced mRNA levels of uncoupling proteins in the Djungarian hamster. Physiol Biochem Zool 74:203–211

24. **Klingenspor M, Ebbinghaus C, Hulshorst G, Stohr S, Spiegelhalter F, Haas K, Heldmaier G** 1996 Multiple regulatory steps are involved in the control of lipoprotein lipase activity in brown adipose tissue. J Lipid Res 37:1685–1695

25. **Wang J, Zhou J, Bondy CA** 1999 IGF1 promotes longitudinal bone growth by insulin-like actions augmenting chondrocyte hypertrophy. FASEB J 13:1985–1990

26. **Eden S** 1979 Age- and sex-related differences in episodic growth hormone secretion in the rat. Endocrinology 105:555–560

27. **Okuma S, Kawashima S** 1980 Spontaneous dwarf rat. Exp Anim 29:301

28. **Wajnrajch MP, Gertner JM, Harbison MD, Chua Jr SC, Leibel RL** 1996 Nonsense mutation in the human growth hormone-releasing hormone receptor causes growth failure analogous to the little (lit) mouse. Nat Genet 12:88–90

29. **Carakushansky M, Whatmore AJ, Clayton PE, Shalet SM, Gleeson HK, Price DA, Levine MA, Salvatori R** 2003 A new missense mutation in the growth hormone-releasing hormone receptor gene in familial isolated GH deficiency. Eur J Endocrinol 148:25–30

30. **Zhou Y, Xu BC, Maheshwari HG, He L, Reed M, Lozykowski M, Okada S, Cataldo L, Coschigamo K, Wagner TE, Baumann G, Kopchick JJ** 1997 A mammalian model for Laron syndrome produced by targeted disruption of the mouse growth hormone receptor/binding protein gene (the Laron mouse). Proc Natl Acad Sci USA 94:13215–13220

31. **Hull KL, Harvey S** 1999 Growth hormone resistance: clinical states and animal models. J Endocrinol 163:165–172

32. **Laron Z** 2002 Growth hormone insensitivity (Laron syndrome). Rev Endocr Metab Disord 3:347–355

33. **Procter AM, Phillips JJA, Cooper DN** 1998 The molecular genetics of growth hormone deficiency. Hum Genet 103:255–272

34. **Binder G** 2002 Isolated growth hormone deficiency and the GH-1 gene: update 2002. Horm Res 58(Suppl 3):2–6

35. **Moseley CT, Orenstein MD, Phillips III JA** 2002 GH gene deletions and IGHD type IA. Rev Endocr Metab Disord 3:339–346

36. **Binder G, Keller E, Mix M, Massa GG, Stokvis-Brantsma WH, Wit JM, Ranke MB** 2001 Isolated GH deficiency with dominant inheritance: new mutations, new insights. J Clin Endocrinol Metab 86:3877–3881

37. **Mullis PE, Deladoey J, Dannies PS** 2002 Molecular and cellular basis of isolated dominant-negative growth hormone deficiency, IGHD type II: insights on the secretory pathway of peptide hormones. Horm Res 58:53–66

38. **McGuinness L, Magoulas C, Sesay AK, Mathers K, Carmignac D, Manneville JB, Christian H, Phillips III JA, Robinson IC** 2003 Autosomal dominant growth hormone deficiency disrupts secretory vesicles *in vitro* and *in vivo* in transgenic mice. Endocrinology 144:720–731

39. **Hayashi Y, Yamamoto M, Ohmori S, Kamijo T, Ogawa M, Seo H** 1999 Inhibition of growth hormone (GH) secretion by a mutant GH-I gene product in neuroendocrine cells containing secretory granules: an implication for isolated GH deficiency inherited in an autosomal dominant manner. J Clin Endocrinol Metab 84:2134–2139

40. **De Vos AM, Ultsch M, Kossiakoff AA** 1992 Human growth hormone and extracellular domain of its receptor: crystal structure of the complex. Science 255:306–312

41. **Cunningham BC, Wells JA** 1989 High-resolution epitope mapping of hGH-receptor interactions by alanine-scanning mutagenesis. Science 244:1081–1085

42. **Borrelli E, Heyman RA, Arias C, Sawchenko PE, Evans RM** 1989 Transgenic mice with inducible dwarfism. Nature 339:538–541

43. **Behringer RR, Mathews LS, Palmiter RD, Brinster RL** 1988 Dwarf mice produced by genetic ablation of growth hormone-expressing cells. Genes Dev 2:453–461

44. **Lin SC, Lin CR, Gukovsky I, Lusis AJ, Sawchenko PE, Rosenfeld MG** 1993 Molecular basis of the little mouse phenotype and implications for cell type-specific growth. Nature 364:208–213

45. **McAndrew SJ, Chen Y, Wiehl P, DiCaprio L, Yun J, Wagner TE, Okada S, Kopchick JJ** 1991 Expression of truncated forms of the bovine growth hormone gene in cultured mouse cells. J Biol Chem 266:20965–20969

46. **Chen WY, White ME, Wagner TE, Kopchick JJ** 1991 Functional antagonism between endogenous mouse growth hormone (GH) and a GH analog results in dwarf transgenic mice. Endocrinology 129:1402–1408

47. **Chen WY, Wight DC, Mehta BV, Wagner TE, Kopchick JJ** 1991 Glycine 119 of bovine growth hormone is critical for growth-promoting activity. Mol Endocrinol 5:1845–1852

48. **Knapp JR, Chen WY, Turner ND, Byers FM, Kopchick JJ** 1994 Growth patterns and body composition of transgenic mice expressing mutated bovine somatotropin genes. J Anim Sci 72:2812–2819

49. **Li Y, Knapp JR, Kopchick JJ** 2003 Enlargement of interscapular brown adipose tissue in growth hormone antagonist transgenic and in growth hormone receptor gene-disrupted dwarf mice. Exp Biol Med (Maywood) 228:207–215

50. **Heldmaier G** 1971 Zitterfreie wärmebildung und körpergröße bei säugetieren. Z Vergl Physiol 73:222–248

51. **Nicholls DG, Rial E** 1999 A history of the first uncoupling protein, UCP1. J Bioenerg Biomembr 31:399–406

52. **Klingenspor M** 2003 Cold-induced recruitment of brown adipose tissue thermogenesis. Exp Physiol 88:141–148

53. **Cummings DE, Clement K, Purnell JQ, Vaisse C, Foster KE, Frayo RS, Schwartz MW, Basdevant A, Weigle DS** 2002 Elevated plasma ghrelin levels in Prader Willi syndrome. Nat Med 8:643–644

54. **Tschop M, Weyer C, Tataranni PA, Devanarayan V, Ravussin E, Heiman ML** 2001 Circulating ghrelin levels are decreased in human obesity. Diabetes 50:707–709

55. **Caminos JE, Seoane LM, Tovar SA, Casanueva FF, Dieguez C** 2002 Influence of thyroid status and growth hormone deficiency on ghrelin. Eur J Endocrinol 147:159–163

56. **Malmlof K, Din N, Johansen T, Pedersen SB** 2002 Growth hormone affects both adiposity and voluntary food intake in old and obese female rats. Eur J Endocrinol 146:121–128